

***In situ* monitoring of galactolipid digestion by infrared spectroscopy in both model micelles and spinach chloroplasts**

Moulay Sahaka^a, Eduardo Mateos-Diaz^a, Sawsan Amara^b, Jutarat Wattanakul^{c,d}, David Gray^c,
Dominique Lafont^e, Brigitte Gontero^a, H el ene Launay^a and Fr ed eric Carri ere^{a*}

^a Aix Marseille Univ, CNRS, UMR7281 Bio energ etique et Ing enierie des Prot eines, 31
Chemin Joseph Aiguier, 13009 Marseille, France.

^b Lipolytech, Zone Luminy Biotech, 163 avenue de Luminy, 13288 Marseille Cedex 09,
France.

^c Division of Food, Nutrition and Dietetics, School of Biosciences, University of Nottingham,
Sutton Bonington Campus, Loughborough, Leicestershire, LE12 5RD, United Kingdom.

^d Department of Food Science and Technology, Faculty of Home Economics Technology,
Rajamangala University of Technology Krungthep, Bangkok, 10120, Thailand

^e Laboratoire de Chimie Organique 2-GLYCO, ICBMS UMR 5246, CNRS-Universit  Claude
Bernard Lyon 1, Universit  de Lyon, b atiment Lederer, 1 rue Victor Grignard, 69622
Villeurbanne Cedex, France

*Corresponding author: Fr ed eric Carri ere; carriere@imm.cnrs.fr

Abstract

Galactolipids are the main lipids from plant photosynthetic membranes and they can be digested by pancreatic lipase related protein 2 (PLRP2), an enzyme found in the pancreatic secretion in many animal species.

Here, we used transmission Fourier-transform infrared spectroscopy (FTIR) to monitor continuously the hydrolysis of galactolipids by PLRP2, *in situ* and in real time. The method was first developed with a model substrate, a synthetic monogalactosyl diacylglycerol with 8-carbon acyl chains (C8-MGDG), in the form of mixed micelles with a bile salt, sodium taurodeoxycholate (NaTDC). The concentrations of the residual substrate and reaction products (monogalactosylmonoglyceride, MGMG; monogalactosylglycerol, MGG; octanoic acid) were estimated from the carbonyl and carboxylate vibration bands after calibration with reference standards. The results were confirmed by thin layer chromatography analysis (TLC) and specific staining of galactosylated compounds with thymol and sulfuric acid.

The method was then applied to the lipolysis of more complex substrates, a natural extract of MGDG with long acyl chains, micellized with NaTDC, and intact chloroplasts isolated from spinach leaves. After a calibration performed with α -linolenic acid, the main fatty acid (FA) found in plant galactolipids, FTIR allowed quantitative measurement of chloroplast lipolysis by PLRP2. A full release of FA from membrane galactolipids was observed, that was not dependent on the presence of bile salts. Nevertheless, the evolution of amide vibration band in FTIR spectra suggested the interaction of membrane proteins with NaTDC and lipolysis products.

Keywords: Enzyme, galactolipase, lipid digestion, pancreatic lipase related protein 2, chloroplast, thin layer chromatography.

Abbreviations: ALA, α -linolenic acid; ATR, Attenuated Total Reflectance; C8-MGDG, monogalactosyl-dioctanoyl glycerol; CRF, chloroplast-rich fraction; DPPC, dipalmitoyl phosphatidylcholine; DW, dry weight; FA, fatty acid; FFA, free fatty acid; FTIR, Fourier-transform infrared spectroscopy; GPLRP2, guinea pig pancreatic lipase related protein 2; LC-MGDG, long chain monogalactosyl-diacyl glycerol; lyso-PC, lysophosphatidylcholine; MGDG, monogalactosyl-diacyl glycerol; MGG, monogalactosyl glycerol; MGMG, monogalactosyl-monoacyl glycerol; NaGDC, sodium glycodeoxycholate; NaTC, sodium taurocholate; NaTDC,; sodium taurodeoxycholate; OA, octanoic acid; PA, palmitic acid; pD, pH in D₂O; PLRP2, pancreatic lipase related protein 2; PUFA, polyunsaturated fatty acid; HDO, semiheavy water; TAG, triacylglycerol; TLC, thin-layer chromatography; TES, N-tris[hydroxymethyl]methyl-2-aminoethane-sulfonic acid;

1. Introduction

Fourier-transform infrared spectroscopy (FTIR) is an effective tool to investigate enzymatic lipolysis and its advantages have already been demonstrated by several studies. The first researchers to attempt to monitor lipolysis using transmission FTIR were Walde and Luisi in 1989. They succeeded in quantifying the substrate consumption and the fatty acids released during the hydrolysis of triacylglycerol (TAG) in reverse micelles, by exploiting the vibration bands of carbonyl (C=O) and C–O bond (Walde and Luisi, 1989). Their method was then successfully applied by O'connor and Cleverly, in 1994, to analyse the activity of bile salt-stimulated lipase on TAG (O'Connor and Cleverly, 1994). Later, FTIR in the mode of Attenuated Total Reflectance (ATR-FTIR) was used to monitor enzymatic lipolysis of TAG films (Snabe and Petersen, 2002) and oil-in-water emulsions (Kaufhold et al., 2014; Khaskheli et al., 2015; Stöbener et al., 2020). FTIR was also used to monitor other lipase-catalyzed reactions such as transesterification for the production of methyl ester (Zagonel et al., 2004; Müller et al., 2010; Natalello et al., 2013) or TAG (Müller et al., 2011).

Previously, we studied the hydrolysis of dipalmitoylphosphatidylcholine (DPPC) by guinea pig pancreatic lipase-related protein 2 (GPLRP2) using transmission FTIR (Mateos-Diaz et al., 2018b). In this last study, we developed a method allowing the simultaneous quantification of residual DPPC and lipolysis products, lysophosphatidylcholine (lyso-PC) and free palmitic acid (PA), by fully exploiting the carbonyl band spectra using calibration curves made with reference standards.

In the present study, our objective was to further develop this approach to investigate the hydrolysis of galactolipids catalyzed by GPLRP2. Galactolipids are the main polar lipids from plant photosynthetic membranes but their digestion was overlooked until enzymes with galactolipase activity like PLRP2 were identified (Sahaka et al., 2020). In a first step, the substrate used was a synthetic monogalactosyl diacylglycerol with 8-carbon acyl chains (C8-

MGDG), presented in the form of mixed micelles with the bile salt sodium taurodeoxycholate (NaTDC). This is a model substrate that we have synthesized and used on several occasions to study the galactolipase activities of various enzymes (Amara, 2011; Amara et al., 2010, 2009; Belhaj et al., 2018; Sahaka et al., 2021). The method was then tested with more complex substrates, including mixed micelles of a natural MGDG with long acyl chains (LC-MGDG), rich in polyunsaturated fatty acids (PUFA), and a chloroplast-rich fraction (CRF) isolated from spinach leaves, in which galactolipids are present in membranes.

2. Materials and methods

2.1. Reagents

MonoGalactosyl Dioctanoyl-Glycerol (C8-MGDG; $M_w=506$ g/mole) was synthesised as previously described (Amara et al., 2009; Lafont et al., 2006; Sias et al., 2004). Natural long chain MonoGalactosyl DiacylGlycerol (LC-MGDG) was purchased from Avanti Polar lipid (ref 840523) (Alabama, USA). With an average molar mass of 752.37 g/mole, LC-MGDG contains α -linolenic acid (18:3; ALA) as the main fatty acid (51%), as well as 16:1 (1%), 16:3 (40%) and 18:2 (8%). ALA, octanoic (OA) and palmitic (PA) acids, Deuterium oxide, Galactose, N-tris[hydroxymethyl]methyl-2-aminoethane-sulfonic acid (TES), Sodium taurodeoxycholate (NaTDC), Sulphuric acid and Thymol were purchased from Sigma-Aldrich (Saint-Quentin Fallavier, France). Calcium chloride (CaCl_2) and sodium chloride (NaCl) were obtained from Euromedex (Souffelweyersheim, France). Acetonitrile, chloroform, ethanol and methanol were all HPLC grade from Carlo Erba (Peypin, France).

2.2. Production and purification of GPLRP2

Recombinant GPLRP2 was produced in *Aspergillus orizae* and purified as previously described (Hjorth et al., 1993). Aliquots (50 μL) of GPLRP2 at 2.3 $\text{mg}\cdot\text{mL}^{-1}$ (or 50 μM) were freeze-dried, resuspended in the deuterated buffer solution used for the reactions, and finally incubated for 48 h at 4°C to reach H/D exchange equilibrium. The aliquots were then kept at -20°C until the reactions were performed. Before being added to the substrates, the aliquots were thawed and diluted to 500 or 1000 nM in D_2O .

2.3. Isolation of CRF from spinach leaves

Spinach leaves, bought from local supermarket, were blanched in hot water at 85 °C for 3 min and then immediately cooled by immersion in an ice-water bath. Blanched spinach leaves

were homogenised in a blender (Waring™) for 30 s with 0.3 M sucrose solution 1:6 (w/v). The homogenate was then filtered through a double-layered cheesecloth. The resulting juice was centrifuged at 10,000 rpm for 10 min at 4 °C. The CRF-containing pellet was freeze-dried for 3–5 days.

2.4. Preparation of micellar solutions of substrates (C8-MGDG, LC-MGDG) and fatty acids (OA, ALA) and CRF suspensions.

Substrates were prepared in the form of mixed micelles with bile salts. Similarly, mixed micelles of free fatty acids (FFAs) were prepared to reproduce the environment of FFAs in the course of the lipolysis reaction in the presence of bile salts. To prepare solutions of C8-MGDG–NaTDC and OA–NaTDC micelles, C8-MGDG and OA were suspended in buffer solutions containing 65.5 mM NaTDC, 500 mM TES buffer, 100 mM NaCl and 5 mM CaCl₂, in D₂O, at pD 8. These buffer conditions were selected after screening various buffers and concentrations and their impact on the IR spectra, especially regarding fatty acid ionization and C8-MGDG phase transition. These optimization steps are described in the Supplementary Materials section with Figure S1 to S6. The suspensions were then heated to 65 °C for 5 min, vortexed and sonicated for 8 min to obtain micelles. C8-MGDG and OA concentrations were both 50 mM and NaTDC to C8-MGDG molar ratio was 1.3. For calibration experiments, a range of dilutions containing 0, 10, 20, 30, 40 and 50 mM of C8-MGDG and OA were prepared using the deuterated buffer solution as diluent.

Following a similar protocol, solutions of LC-MGDG–NaTDC and ALA–NaTDC micelles were prepared in buffer solutions containing 30 mM NaTDC, 200 mM TES buffer, 100 mM NaCl and 5 mM CaCl₂, in D₂O, at pD 8. LC-MGDG and ALA concentrations were 22.5 and 15 mM, respectively, and NaTDC/MGDG molar ratio was 1.3. For calibration experiments, a

range of dilutions containing 0, 3, 6, 9, 12 and 15 mM of ALA was prepared using the deuterated buffer solution as diluent.

Freeze-dried CRF was suspended in the same deuterated buffer solution at a concentration of 100 g/L, in the absence and presence (30 mM) of NaTDC.

LC-MGDG–NaTDC micelles and CRF suspensions were also prepared in H₂O for lipid extraction and analysis by TLC.

2.5. Analysis of MGDGs and CRF lipolysis by T-FTIR

Lipolysis experiments were carried out by adding 5 μL of rGPLRP2 solution (500 or 1000 nM) to 45 μL of substrate dispersions (C8-MGDG micelles, LC MGDG micelles or CRF suspensions) to obtain 50 or 100 nM final enzyme concentration. The reaction mixtures were placed and squeezed between two CaF₂ transmission crystals with a 50 μm polytetrafluoroethylene (Teflon) spacer. IR-spectra were then recorded each 5 min during 2 h at 37 °C using a JASCO™ FT/IR-6100 Fourier-transform infrared spectrometer. The sample chamber was continuously purged with a flow of dry air to avoid the presence of water vapour and the formation of semiheavy water (HDO) molecules in the sample. All the spectra are an average of 128 scans, with 4 cm⁻¹ of resolution, apodized with a cosine function.

2.6. Estimation of residual substrate and lipolysis product concentrations during C8-MGDG hydrolysis using FTIR absorbance

Upon lipolysis, a C8-MGDG molecule can be converted in monogalactosyl monoctanoylglycerol (C8-MGMG) and a free OA. To quantify these compounds from IR absorbance, we used equations (1), (2) and (3). The matrix system (1) with 3 equations and 3 unknowns was adapted from the previous study on phospholipid hydrolysis by Mateos-Diaz et al. (Mateos-Diaz et al., 2018b). It allows estimating the concentrations of the residual

substrate and lipolysis products based on the absorbances of the reaction mixture at 3 different wavenumbers.

$$\begin{bmatrix} A_{1744} \\ A_{1722} \\ A_{1682} \end{bmatrix} = \begin{bmatrix} \epsilon_{C8-MGDG}^{1744} & \epsilon_{C8-MGMG}^{1744} & \epsilon_{OA}^{1744} \\ \epsilon_{C8-MGDG}^{1722} & \epsilon_{C8-MGMG}^{1722} & \epsilon_{OA}^{1722} \\ \epsilon_{C8-MGDG}^{1682} & \epsilon_{C8-MGMG}^{1682} & \epsilon_{OA}^{1682} \end{bmatrix} \times \begin{bmatrix} [C8-MGDG] \\ [C8-MGMG] \\ [Free OA] \end{bmatrix} \quad (1)$$

$$[Free OA] = A_{1553} / \epsilon_{OA}^{1553} \quad (2)$$

$$[Free OA] = A_{1408} / \epsilon_{OA}^{1408} \quad (3)$$

With A_i : absorbance at wavenumber $i \text{ cm}^{-1}$, ϵ_x^i : molar extinction coefficient ($\text{M}^{-1} \text{ cm}^{-1}$) of compound x at wavenumber $i \text{ cm}^{-1}$, $[x]$: concentration (M) of compound x .

2.7. Estimation of free fatty acid (FFA) concentration during LC-MGDG and CRF hydrolysis using FTIR absorbance

To quantify FFA during lipolysis of LC-MGDG–NaTDC micelles and CRF suspensions (with and without NaTDC), we used equations (4) and (5).

$$[FFA] = A_{1555} / \epsilon_{ALA}^{1555} \quad (4)$$

$$[FFA] = A_{1407} / \epsilon_{ALA}^{1407} \quad (5)$$

2.8. Calibration of FTIR absorbance versus concentration of C8-MGDG, C8-MGMG, OA and ALA.

For calibration, C8-MGDG–NaTDC, OA–NaTDC, and ALA–NaTDC micellar solutions were diluted with the buffer solutions in which they were prepared to obtain a concentrations range of 0, 10, 20, 30, 40 and 50 mM for C8-MGDG and OA and of 0, 3, 6, 9, 12 and 15 mM for ALA. FTIR spectra of these calibration solutions were then recorded under the same conditions as the lipolysis experiments.

For C8-MGMG calibration, no commercial or synthetic standard was available. To produce it, the mixed micelles of C8-MGDG–NaTDC were hydrolyzed by GPLRP2 (100 nM), at 37°C. The reaction was stopped after 1 h of incubation to make sure that C8-MGDG disappeared completely and that there was enough accumulation of C8-MGMG. To stop the lipolysis, the reaction mixture was heated at 90 °C for 10 min to denature GPLRP2. The concentration of C8-MGMG in the hydrolysate (26 mM) was estimated by TLC-densitometry using the specific staining of galactose with thymol/sulfuric acid, as previously reported (Sahaka et al., 2021). A range of dilutions (1 to 5-fold) of the hydrolysate was prepared and their spectra were recorded at 37 °C. In these spectra, the carbonyl vibration band combines absorbance of C8-MGMG with that of free OA (Figure S7A). Some monogalactosyl glycerol (MGG) was formed that could not interfere with the vibration bands of carbonyl (C=O) bond. The carboxylate vibration band, on the other hand, is composed only of the absorbance of free OA (Figure S7A). This band allowed us to estimate free OA concentrations in the hydrolysate dilution range (14, 28, 42, 54, and 72 mM OA) with high accuracy, using equation (2). OA-NaTDC micellar solutions were then prepared at the same concentrations. Their spectra were recorded (Figure S7B) and subtracted from the spectra of the hydrolysate at the same dilution (Figure S7C). The latter were thus cleared of OA absorbances and used for calibration of C8-MGMG (Figure S7C).

All calibration curves are presented in Figure S7.

2.9. FTIR spectra treatment

All spectra presented in this study were submitted to baseline and water vapor corrections.

All "raw" spectra presented were subjected to subtraction of the buffer solutions spectra to present only the absorbance of lipids or CRFs.

Difference spectra were made by subtracting the initial spectrum from the reaction spectra at various times. In the case of C8-MGDG and LC-MGDG hydrolysis, this initial spectrum corresponds to the substrate spectrum without enzyme. In the case of CRF lipolysis, it corresponds to the spectrum recorded 5 min after the addition of enzyme. The spectrum of CRF without enzyme could not be used as initial spectrum because CRF spectra are not strictly reproducible in intensities because we were dealing with dispersions that form deposits in absence of continuous agitation.

The absorbance of HDO molecules was removed from the reaction spectra (raw and difference) by subtracting a model HDO spectrum from them. This model HDO spectrum was obtained by subtracting a pure D₂O spectrum from a hydrated one. The hydration was induced either by adding a very small amount of water or by leaving the D₂O in contact with the room air. Before being subtracted, the model HDO spectrum was multiplied by a coefficient α to match the hydration level of the spectrum to correct. This coefficient α was estimated using the equation (6).

$$A_{\text{spectrum to correct}}^{1452} = \alpha \cdot A_{\text{HDO}}^{1452} \quad (6)$$

With $A_{\text{spectrum to correct}}^{1452}$: Absorbance at 1452 cm⁻¹ of the spectrum to correct,

and A_{HDO}^{1452} : Absorbance of the HDO model spectrum at 1452 cm⁻¹.

All these treatments were performed using the software Spectra Manager® version V.2.07.

2.10. Analysis of C8-MGDG lipolysis by thin-layer chromatography (TLC) and densitometry

A GPLRP2 aliquot (1000 nM) was added to C8-MGDG–NaTDC micelles to obtain a 100 nM enzyme concentration, in D₂O, at 37 °C. The reaction volume was 200 μ L. Aliquots of 25 μ L were collected at different reaction times (0, 10, 20, 50, 90 and 120 min) and immediately mixed with 1 mL of a stop solution containing 200 mM HCl and 150 mM NaCl. Substrates

and reaction products in aliquots were extracted and analysed using TLC- densitometry and thymol-sulfuric acid reagent, as previously described (Sahaka et al., 2021), and a mixture of chloroform/methanol/water (25/15/1.25, v/v/v) for elution.

2.11. Analysis of LC-MGDG and CRF lipolysis by TLC

GPLRP2 aliquots (500 nM) were added to LC-MGDG–NaTDC micelles and CRF suspensions (with and without NaTDC) to obtain 50 nM enzyme concentration, in H₂O, at 37 °C. Aliquots of 25µL were collected after 1h incubation and immediately mixed with 1 mL of stop solution. Substrates and reaction products in aliquots were extracted and analysed using TLC, as previously described (Sahaka et al., 2021), and a mixture of chloroform/methanol/water (47.5/10/1.25, v/v/v) for elution of long chain galactolipids (Wattanakul et al., 2019).

3. Results

3.1. FTIR spectra of C8-MGDG, LC MGDG, CRF, octanoic acid, palmitic acid and α -linolenic acid.

Figure 1A shows FTIR spectra of pure C8-MGDG, LC-chain MGDG, OA, ALA and PA, and CRFs, in the presence of NaTDC, at pD 8 and 37 °C.

In all spectra, the region between 3040 and 2813 cm⁻¹ (Figure 1 B) is dominated by two large peaks attributed to symmetric (ν_s CH₂) and asymmetric (ν_{as} CH₂) methylene stretching vibrations, both peaks have a shoulder corresponding to symmetric (ν_s CH₃) and asymmetric (ν_{as} CH₃) vibrations of terminal CH₃ groups, respectively (Snyder et al., 1982). In the same region, ALA, LC-MGDG and CRF spectra have in addition a peak corresponding to alkenyl

C-H stretching vibration ν_{CH} (Figure 1 B) (Vlachos et al., 2006), indicating the presence of C=C double bonds.

Between 1800 and 1640 cm^{-1} all spectra present a band (Figure 1C) attributed to carbonyl stretching vibration $\nu_{\text{C=O}}$ (Blume et al., 1988; Levin et al., 1982; Lewis and McElhaney, 1993; Mateos-Diaz et al., 2018a; Yan et al., 2000). In the case of the CRF spectrum, this carbonyl band is globally attributed to chloroplast membrane lipids.

Between 1600 cm^{-1} and 1350 cm^{-1} , ALA and OA spectra show two peaks (Figure 1D), attributed to the symmetric ($\nu_{\text{s}}\text{COO}^-$) and asymmetric ($\nu_{\text{as}}\text{COO}^-$) carboxylate stretching vibrations (Mizuguchi et al., 1997). In the case of palmitic acid (PA), $\nu_{\text{s}}\text{COO}^-$ and $\nu_{\text{as}}\text{COO}^-$ occur as doublets (Figure 1D). The splitting of carboxylate vibrations into doublets has previously been reported in the spectra of carboxylate-calcium complexes and has been attributed to the coexistence of different structural organizations (Mielczarski et al., 1993a, 1993b). Between its two doublets, PA present a band (Figure 1D) attributed to CH_2 scissoring vibration ($\nu_{\text{sci}}\text{CH}_2$) (Wieser and Danyluk, 1972).

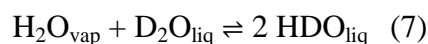
Panel E of Figure 1 shows vibrations characteristic of proteins in the CRF spectrum. Between 1700 and 1600 cm^{-1} , there is a large band corresponding to deuterated amides I (amide I'). The shoulder between 1590 and 1540 cm^{-1} was attributed to the vibrations of non-deuterated amides II. The large band between 1500 and 1400 cm^{-1} corresponds to the vibrations of deuterated amides II (amide II') (Goormaghtigh et al., 1994; de Jongh et al., 1997; Barth and Zscherp, 2002).

3.2. Monitoring of C8-MGDG hydrolysis using FTIR spectroscopy

Hydrolysis of C8-MGDG–NaTDC micelles, by GPLRP2 (50 and 100 nM), in D_2O was performed at pD 8 and 37° C in the transmission cell of the FTIR spectrophotometer. IR

spectra were recorded every 5 minutes for 2 hours, in the presence and in absence (blank) of GPLRP2.

In the absence of enzyme (Figure 2 A), no change with time is visually noticeable in the raw spectra of C8-MGDG. However, by subtracting the initial spectrum ($t = 0$ min) from the other spectra/times, an increase in absorbance at 1451 cm^{-1} (Figure 2A') is revealed, that can be attributed to the scissoring vibration of HDO molecules (δHDO) (Ceccaldi et al., 1956). The appearance of HDO results from the hydration of liquid D_2O by the atmospheric H_2O vapor, according to equation (7). This phenomenon occurs despite a continuous purge of the sample with dry air.



In the presence of enzyme, important changes in the raw and difference spectra of C8-MGDG are observed over time (Figure 2 B and B'). Changes related to HDO production were suppressed in these spectra in order to present only the evolutions induced by the enzyme. The hydrolysis was manifested in raw spectra by a progressive disappearance of the $\nu\text{C}=\text{O}$ band of C8-MGDG (at around 1744 cm^{-1}) giving rise to $\nu\text{C}=\text{O}$ bands of C8-MGMG and protonated free OA (Figure 2 B). We also observe the appearance of two imposing peaks corresponding to the $\nu_{\text{as}}\text{COO}^-$ and $\nu_{\text{s}}\text{COO}^-$ vibrations of ionized free OA carboxylate (Figure 2 B). The difference spectra shows a decrease in absorbance at 1744 cm^{-1} and an increase in absorbance at 1682 , 1553 and 1408 cm^{-1} attributed to the disappearance of $\nu\text{C}=\text{O}$ band of C8-MGDG, and the appearance of $\nu\text{C}=\text{O}$, $\nu_{\text{as}}\text{COO}^-$ and $\nu_{\text{s}}\text{COO}^-$ bands of OA, respectively (Figure 2 B').

To monitor quantitatively the reaction products using $\nu\text{C}=\text{O}$ vibrations, absorbances at 1744 cm^{-1} , 1722 cm^{-1} , and 1682 cm^{-1} were extracted from the raw spectra. These wavenumbers correspond to the absorption maxima of C8-MGDG (Figure 3A), C8-MGMG (Figure 3B) and

free OA (Figure 3C) carbonyl bands, respectively. For each reaction time, C8-MGDG, C8-MGMG and OA concentrations were estimated from these absorbances using the matrix system (1) with 3 equations and 3 unknowns adapted from the study on phospholipid hydrolysis by Mateos-Diaz et al. (Mateos-Diaz et al., 2018b).

To monitor quantitatively the reaction products using carboxylate vibrations, we extracted absorbances at 1553 cm^{-1} and 1408 cm^{-1} , corresponding to maxima of $\nu_{\text{as}}\text{COO}^-$ (Figure 3E) and $\nu_{\text{s}}\text{COO}^-$ (Figure 3F) from the difference spectra. Free OA concentrations were then estimated from these absorbances using equations (2) and (3).

The resolution of equations (1), (2) and (3) requires to determine the molar extinction coefficients of C8-MGDG, C8-MGMG and OA. For this purpose, carbonyl and carboxylate band spectra of C8-MGDG (Figure 3A), C8-MGMG (Figure 3B) and OA (Figure 3C, E and F) were recorded at different concentrations, under the same conditions as the lipolysis reactions. These spectra were used to draw calibration curves at the wavenumbers relevant for reaction monitoring (Figure S2 A, B, C and D). Table 1 shows the molar extinction coefficients estimated from these calibration curves.

Figure 4 shows the evolution with time of the lipolysis reaction of C8-MGDG in the presence of 100 nM (Figure 4 A) and 50 nM GPLRP2 (Figure 4 C). Disappearance of the initial C8-MGDG substrate is shown, while the lipolysis products C8-MGMG, monogalactosylglycerol (MGG) and free OA appear. Their respective concentrations were estimated from the IR spectra, C8-MGDG is fully hydrolysed after 20 min with 50 nM GPLRP2 and after 120 min with 100 nM GPLRP2. Free OA concentrations estimated using the absorbances at 1682 , 1553 and 1408 cm^{-1} are similar and increase continuously for 2 hours of reaction. C8-MGMG initially accumulated and then gradually disappeared, with maximum accumulation at 80 min (Figure 4 C) and 20 min (Figure 4 A) in the presence of 50 nM and 100 nM GPLRP2, respectively. During the C8-MGMG accumulation phase, its production was correlated with

C8-MGDG consumption and free OA production. Further hydrolysis of C8-MGMG began only when its quantity reached 4 times that of MGDG, i.e. 80% lipolysis of MGDG, regardless the amount of enzyme present. The late release of OA was mostly correlated with C8-MGMG hydrolysis.

C8-MGMG hydrolysis indicates the production of MGG (Figure 9). However, as no band was assigned to MGG in the FTIR spectra, its quantification was not possible. MGG concentrations shown in Figure 4 A and C were deduced from those of C8-MGDG, C8-MGMG and OA, using equation (8).

$$[MGG] = [C8-MGDG]_{initial} - [C8-MGDG] - [MGMG] \quad (8)$$

With $[C8-MGDG]_{initial}$: concentration of C8-MGDG at 0 minute incubation time.

3.3. Monitoring of C8-MGDG hydrolysis using TLC and densitometry

To validate the results obtained by FTIR spectroscopy, we also analysed the lipolysis of C8-MGDG–NaTDC micelles, by 100 nM GPLRP2, using TLC-densitometry and thymol-sulfuric acid derivatization (Figure 4B). Thymol-sulphuric acid reagent allowed to quantify only galactosylated compounds (C8-MGDG, C8-MGMG and MGG). OA concentrations were calculated from C8-MGMG and MGG concentrations, using equation (9).

$$[OA] = [C8-MGMG] + 2. [MGG] \quad (9)$$

Concentrations and kinetic curves obtained from TLC analysis (Figure 4B) are very similar with those obtained using FTIR spectroscopy and the same concentration of enzyme (Figure 4 A). The specific activities of GPLRP2 estimated from both methods using 100 nM GPLRP2 are very close (FTIR: 981 ± 97 U/mg, TLC-densitometry: 727 ± 67 U/mg; with 1U = 1 μ mole of FFA released per min; see Table 2). However, the specific activity is reduced to 439 ± 125 U/mg using 50 nM GPLRP2, which indicates that the assay conditions are not fully optimized to measure a constant specific activity when varying the enzyme amount.

3.4. Monitoring of LC-MGDG hydrolysis using FTIR spectroscopy

Lipolysis of LC-MGDG–NaTDC micelles, by 50 nM GPLRP2, in D₂O, at pD 8 and 37° C, was studied using IR spectroscopy. Spectra were recorded every 5 minutes for 2 hours, in presence and in absence of GPLRP2.

In the absence of enzyme, only the production of HDO molecules was observed in the difference spectra (spectra not shown), as previously observed during the incubation of C8-MGDG without enzyme (Figure 2 A').

In the presence of enzyme, the raw and difference spectra (Figure 2 C and C') show the same changes as those observed during the hydrolysis of C8-MGDG (Figure 2 B and B'). Carboxylate vibrations ($\nu_{\text{as}}\text{COO}^-$ and $\nu_{\text{s}}\text{COO}^-$) of released fatty acids appear as two peaks as in the spectrum of ALA-NaTDC (Figure 1D), this is consistent with the fact that ALA is the main fatty acid in LC-MGDG (60 % w/w of total FA) (Amara et al., 2010).

FFA concentration in the reaction medium over time was estimated from a calibration established with ALA. Carbonyl and carboxylate band spectra of ALA (Figure 3G and H) were recorded at different concentrations, under the same conditions as the lipolysis reactions. These spectra were used to draw calibration curves at the wavenumbers relevant for reaction monitoring: 1555 cm⁻¹ for $\nu_{\text{as}}\text{COO}^-$ and 1408 cm⁻¹ for $\nu_{\text{s}}\text{COO}^-$ (Figure S2 E). FFA concentrations were estimated from absorbances at these wavenumbers using equations (4) and (5) and the molar extinction coefficients estimated from the calibration curves (Table 1).

Figure 4 D shows FFA concentrations over time estimated by this method. The concentrations estimated from absorbances at 1555 cm⁻¹ and 1407 cm⁻¹ were found to be identical. The FFA concentration reached after 120 min (27 mM; Figure 4D) corresponds to a lipolysis level of

60%, taking into account a substrate concentration of 22.5 mM and the possibility to release two fatty acid molecules from LC-MGDG. For the sake of comparison, the FFA concentration reached after 120 min with C8-MGDG and the same enzyme concentration (50 nM) was 2-fold higher (61 mM; Figure 4C) than the concentration reached upon LC-MGDG lipolysis. However, the initial concentration in the C8-MGDG substrate was also higher (50 mM) and this level of FFA corresponds to a lipolysis level of 61 % that is the same as with LC-MGDG. Similarly, the specific activity estimated for GPLRP2 acting on LC MGDG (492 ± 30 U/mg) is in the same range as the specific activity measured with C8-MGDG (439 ± 125 U/mg; see Table 2), at the same enzyme concentration (50 nM).

3.5. Monitoring of CRF lipolysis using FTIR spectroscopy

We then studied whether GPLRP2 was able to get access to galactolipids and hydrolyze them when they are present in the photosynthetic membranes of the chloroplast. Lipolysis of CRF was performed using 50 nM GPLRP2 in D₂O, at pD 8 and 37 °C, without and with bile salts (NaTDC) to reproduce digestive conditions in the gastrointestinal tract. FTIR spectra of CRF suspension were recorded every 5 min during two hours.

Changes in the CRF spectra over time were too weak to be visible on the raw spectra (see Figure S9). They were revealed and analysed by establishing the difference spectra (Figure 5).

In absence of enzyme and presence of NaTDC, we observed an important decrease in absorbance that extends from 1700 to 1350 cm⁻¹ (Figure 5 A). This decrease is composed of two large bands, that we attributed to amide I' (between 1700 and 1600 cm⁻¹) and amide II' (between 1500 and 1350 cm⁻¹) vibrations, and a third less important band that could correspond to amide II vibrations (between 1600 and 1500 cm⁻¹). This phenomenon was not observed without NaTDC (Figure 5 A') and was therefore related to the presence of this surfactant. Surfactants are known to bind to protein complexes in chloroplast membranes and

solubilise them (Bril et al., 1969; Yu et al., 2014). Therefore, the decrease in amide absorbances could correspond to protein solubilisation, more precisely to the formation of proteins-NaTDC complexes. To investigate this hypothesis, we incubated CRF with other surfactants: sodium glycodeoxycholate (NaGDC), sodium taurocholate (NaTC) and the non-ionic surfactant Triton X-100, whose ability to disturb chloroplast membranes has already been observed and established (Yu et al., 2014). Similar decreases in absorbance were observed with all surfactants tested, with differences in intensity (Figure S10). This reinforces the hypothesis of changes in CRF membranes by NaTDC. We also observed that the presence of NaTDC shifted the asymmetric vibrations of the C-H bonds ($\nu_{as}CH_2$ and $\nu_{as}CH_3$) towards higher wavenumbers (Figure 6A). This shows that the presence of NaTDC increases the acyl chain mobility in CRF membranes. However, the membrane disturbance is probably limited because the microscope observation of CRF dispersed with NaTDC showed non-disintegrated chloroplasts (Figure 6B), which appear similar to those observed in intact cells from spinach leaves (Figure 6C).

In the presence of NaTDC and GPLRP2 (Figure 5B), we observe the same decrease in protein absorbance as with NaTDC alone but additional changes resulting from the lipolysis by GPLRP2 also appeared. To isolate these last ones, the spectra in absence of enzyme (Figure 5A) were subtracted from those in presence of enzyme (Figure 5B). The differential spectra obtained (Figure 5C) are very similar to those recorded in the course of LC-MGDG hydrolysis (Figure 2 C'). They show a decrease in absorbance of lipids $\nu_{C=O}$ vibrations at 1741 cm^{-1} and the appearance of carboxylate peaks (ν_sCOO^- and $\nu_{as}COO^-$) of released fatty acids at 1556 and 1405 cm^{-1} . We also observed a decrease in absorbance between 1700 and 1600 cm^{-1} (minimum at 1646 cm^{-1} ; Figure 5 C) which did not appear during the hydrolysis of LC MGDG. We attributed it to the vibrations of amides I'. This could be due to an increase in proteins-NaTDC interaction caused by the disappearance of galactolipids linked to proteins,

or to novel interactions of lipolysis products with proteins. Indeed, lyso-galactolipids like MGMG and DGMG are also surfactants.

The lipolysis reaction was monitored by quantifying the released fatty acids. The concentration of FFA was estimated from the absorbances at 1556 and 1405 cm^{-1} , corresponding to $\nu_{\text{s}}\text{COO}^-$ and $\nu_{\text{as}}\text{COO}^-$ peaks, using equations (4) and (5). After 2 h of reaction, a concentration of 5.3 mM FFA (ALA equivalent) was reached, which corresponds to the release of 71% of the fatty acids of chloroplast galactolipids (Figure 7 A). This percentage has been estimated by considering that (1) there are 28.59 mg and 25.81 mg of MGDG and DGDG per g of spinach CRF (DW) (Wattanakul et al., 2019) and (2) the MGDG and DGDG of spinach leaves contain 71% and 58% (w/w) of FA (Amara et al., 2010). We could estimate a specific activity of 89 ± 7 U/mg that is about two times less than the one obtained with LC-MGDG (166 ± 9 U/mg) in the presence of NaTDC (see Table 2).

Given the effects of bile salts on CRF, we wondered whether their action could favour the activity of GPLRP2 on the membrane galactolipids. The hydrolysis of CRF by 50 nM GPLRP2 was therefore tested in the absence of NaTDC.

The raw spectra of CRF were larger in absence (Figure S9 A' and B') than in the presence of NaTDC (Figure S9 A and B). This is consistent with our hypothesis that NaTDC causes a decrease in the absorbance of membrane protein bands. However, as before in the presence of NaTDC, changes with time on the raw spectra were difficult to observe because of their low intensity. Again, the spectra evolutions could be revealed and analysed using the difference spectra (Figure 5).

In absence of NaTDC and GPLRP2 (Figure 5 A'), the difference spectra did not show the large decrease in absorbance due to NaTDC and observed in Figure 5A. There were however rather small decrease and increase in absorbance at 1530 and 1442 cm^{-1} , which we attributed

to the disappearance of amides II and the appearance of amides II', respectively. The increase in absorbance at 1442 cm^{-1} may also be due in part to the appearance of HDO molecules.

In presence of GPLRP2 (Figure 5 B'), we observed the same variations as in the absence of GPLRP2, mixed with the classical variations attributed to lipolysis (disappearance of galactolipid carbonyls at 1741 cm^{-1} and appearance of FFA carboxylates at 1560 and 1405 cm^{-1}). We also observed bands appearing between 1700 and 1600 cm^{-1} which we attributed to amide I' vibrations (Figure 5 B'). Four peaks are observed at 1704 , 1683 , 1648 and 1617 cm^{-1} . The peaks at 1704 and 1683 cm^{-1} may correspond more precisely to β turn structures and the peaks at 1648 and 1617 cm^{-1} to random coil and β sheet structures of proteins (Kong and Yu, 2007). The peak at 1683 cm^{-1} may also be partly composed of the $\nu\text{C}=\text{O}$ vibrations of FFA as observed in the difference spectra of C8-MGDG and LC-MGDG hydrolysis (Figure 2 B' and C'). The increase in absorbance of amides I' bands may have been caused by the disappearance of proteins-galactolipids interactions and/or the appearance of interactions between proteins and other compounds, such as the proteins themselves or the lipolysis products (lyso-galactolipids and FFA).

To observe only the changes caused by lipolysis, the spectra in absence of enzyme were subtracted from those in presence of enzyme. This greatly reduced the changes due to amide II' appearance and amide II disappearance and made the carboxylates peaks more quantitative (Figure 5 C'). The quantitative analysis of the reaction consisted of monitoring the concentration of fatty acid released. FFA concentration was estimated from the two carboxylate peaks ($\nu_{\text{s}}\text{COO}^-$ and $\nu_{\text{as}}\text{COO}^-$) using equations (4) and (5). The FFA concentrations (Figure 7 B) and the specific activity obtained ($133 \pm 29\text{ U/mg}$; Table 2) was more important than in the presence of NaTDC ($89 \pm 7\text{ U/mg}$, see Table 2). After 2 h of reaction, the estimated amount of FFA was equivalent to the total amount of fatty acids present in chloroplast galactolipids (Figure 7 B). It is worth noticing, however, that the calibration curve

for ALA measurement was performed with ALA-NaTDC micelles, as in the previous experiment performed with NaTDC. Since the interaction of ALA with NaTDC may change the molar extinction coefficient of ALA, it is possible that we have overestimated or underestimated the amounts of ALA equivalents released during the lipolysis of CRF in the absence of NaTDC. We had however no obvious alternative because ALA is insoluble in water and NaTDC micelles allow dispersing it.

3.6. Analysis of LC-MGDG and CRF lipolysis using TLC

To validate FTIR analysis of galactolipids and CRF lipolysis by GPLRP2, lipolysis reactions were reproduced in water instead of D₂O and the lipolysis products were extracted and analyzed by thin-layer chromatography coupled to densitometry after staining of galactolipids with thymol/sulfuric acid reagent. Figure 8A shows the TLC separation of the lipolysis products generated upon hydrolysis of LC-MGDG by GPLRP2 in the presence of NaTDC. In the absence of enzyme, only the LC MGDG band is observed in the form of a doublet. After 1 h of incubation with GPLRP2, the latter has almost disappeared and novel bands appear in the organic phase resulting from the extraction: a lower red band that can be attributed to MGG (Sahaka et al., 2021) and two upper bands corresponding to less polar compounds that can be attributed to FFA. When compared to the ALA standard loaded on the same plate, one can see that the yellow band corresponds to free ALA. This is the first time that we observed this ALA yellow staining by the thymol-sulphuric acid reagent. The separate analysis of the aqueous phase resulting from the extraction shows the appearance of MGG, also stained in red by the thymol-sulphuric acid reagent. Therefore, all the lipolysis products identified by FTIR can be seen by TLC analysis.

The action of GPLRP2 on CRF dispersions, in the presence and absence of NaTDC, was also analysed using TLC (Figure 8B). Without the enzyme, CRF showed two large red bands

attributed to MGDG and DGDG (Sahaka et al., 2021; Wattanakul et al., 2019). After 1 h incubation with GPLRP2 at 37 °C, in the presence and absence of NaTDC, MGDG and DGDG bands have almost disappeared and MGMG and free ALA bands appeared (Figure 8). The weakness of MGMG band and the absence of DGMG band indicates that these intermediate lipolysis products have also been hydrolysed to a large extent, which is in agreement with the FTIR analysis. Qualitatively the reaction appears to be more advanced in the presence of NaTDC than in its absence.

4. Discussion

4.1 Monitoring galactolipid lipolysis by FTIR

Previously, we monitored the lipolysis of DPPC-NaTDC micelles by GPLRP2, in D₂O, using T-FTIR. We used the composite carbonyl band to estimate the concentration of DPPC, lysoPC and palmitic acid (PA) throughout the reaction (Mateos-Diaz et al., 2018b). In the present study, we used the same method to monitor the hydrolysis of a medium chain galactolipid, C8-MGDG, also presented in the form of mixed micelles with NaTDC. We quantified the residual substrate (C8-MGDG) and reaction products (C8-MGMG and OA) by exploiting the carbonyl band, as previously. The final reaction product, MGG, was estimated from the contents in residual MGDG, MGMG, OA and the reaction stoichiometry. The C8-MGMG standard used for calibration was produced by hydrolysing C8-MGDG with GPLRP2. This allowed to obtain a perfect match between the concentration of C8-MGMG estimated and that expected from C8-MGDG disappearance and OA release. We also used the carboxylate bands to quantify FFA (OA), what was not attempted before. The concentrations obtained with these peaks were the same as those obtained with the carbonyl band. Then, in order to validate the FTIR results, the reaction, carried out in D₂O, was also monitored with

TLC-densitometry analysis of lipolysis products. This allowed to estimate similar reaction rates and product concentrations with both methods.

4.2 Substrate specificity and specific activity of GPLRP2

During lipolysis of C8-MGDG and NaTDC mixed micelles, the disappearance of the intermediate lipolysis product C8-MGMG and the production of MGG deduced from FFA release shows that GPLRP2 can hydrolyse the two ester functions in C8-MGDG and confirms our previous studies using TLC analysis (Sahaka et al., 2021). This means that GPLRP2 can attack at both sn-1 and sn-2 positions of C8-MGDG, or, that after the hydrolysis of sn-1 position, an intramolecular migration of the remaining acyl chain from the sn-2 to sn-1 position occurs, followed by a second hydrolysis at this position (Figure 9). Since GPLRP2 has been described in several studies as an enzyme preferring the sn-1 position (Carrière et al., 1998; Fauvel et al., 1981; Mateos-Diaz et al., 2018b; Withers-Martinez et al., 1996), the latter hypothesis is the one we consider most likely. However, in a study using synthetic glycerophosphatidylcholines containing α -eleostearic acid, either at the sn-1 position or at the sn-2 position and a nonhydrolyzable ether bond at the other position to prevent acyl chain migration during lipolysis, it was shown that GPLRP2 could release α -eleostearic acid from the sn-2 position (phospholipase A2 activity) at a rate that was 10-fold lower than the rate of α -eleostearic acid release from the sn-1 position (phospholipase A1 activity) (El Alaoui et al., 2016). Therefore, some of the FFA released from galactolipids by GPLRP2 may also be generated by a direct attack of the sn-2 position.

T-FTIR was also used to monitor the hydrolysis of a natural LC-MGDG, solubilized in mixed micelles with NaTDC, by GPLRP2. The spectra evolved in the same way as those of C8-MGDG, showing that this technique is applicable to natural lipids having a heterogeneous fatty acid composition. However, due to the lack of MGMG standard for calibration, we could

not quantitatively exploit the carbonyl band and we only quantified the FFA from the carboxylate bands using ALA as a reference standard (Figure 4D).

The specific activities of GPLRP2 obtained with LC-MGDG and C8-MGDG were similar (Table 2). These data confirm the previous study by Amara et al. (Amara et al., 2010) showing that the galactolipase activity of PLRP2 is poorly affected by acyl chain length and/or degree of unsaturation. Assay conditions were however quite different with FFA estimated from continuous pH-stat titration under strong mechanical stirring of the substrate micellar dispersion. Higher specific activities reaching 5000 U/mg were recorded under these conditions. Nevertheless, FTIR analysis can be performed in a much smaller volume (50 μ L versus 5 to 15 mL) which allows using low amounts of rare natural substrates.

4.3 Specific activity of GPLRP2 in D₂O versus H₂O

The specific activity of GPLRP2 on C8-MGDG in D₂O was estimated from the release of octanoic acid during the first 10 min of the reaction and expressed in μ moles of fatty acid released per min and per mg of enzyme (or U/mg). The values obtained were 727 ± 67 U/mg by FTIR and 981 ± 97 U/mg by TLC analysis (Table 2). These activities were similar but 2 to 2.7-fold lower than the activity (1945 ± 116 U/mg) obtained when studying the same reaction in H₂O under similar conditions and the same enzyme concentration (Sahaka et al., 2021). This finding is in line with our previous study on DPPC lipolysis by GPLRP2, in which we also found a lower rate of lipolysis in D₂O compared to H₂O (Mateos-Diaz et al., 2018b). A difference was also observed between the hydrolysis of C8-MGMG in D₂O and that in H₂O. In water, the hydrolysis started as soon as C8-MGMG appeared (Sahaka et al., 2021), whereas in D₂O it only started when the amount of C8-MGDG reached 4 times that of the residual C8-MGDG, independently of the amount of enzyme present (Figure 4). Therefore, the lower

hydrolytic activity of GPLRP2 in D₂O compared to water can be generalized. Moreover, the nature of the solvent may also influence the substrate preference of GPLRP2.

4.4 Monitoring galactolipid lipolysis by FTIR in the complex environment of the chloroplast

T-FTIR was used to monitor the action of GPLRP2 on CRF. Although this natural material presents a low mass concentration of galactolipid (54 mg/g CRF (DW) (Wattanakul et al., 2019)), it was possible to observe the hydrolysis of chloroplast membrane lipids in differential spectra. The previous data obtained with model galactolipid substrates allowed identifying the spectral region of interest, and the lipolysis of CRF was monitored by quantifying FFA over time using the carboxylate peaks. Bile salts (NaTDC) were initially added to favour the action of GPLRP2 on membrane galactolipids since the optimum activity of GPLRP2 on purified galactolipids was observed in the presence of bile salts (Amara et al., 2010, 2009). About 70% of the CRF galactolipid fatty acids were released after 2 h of incubation under these conditions (Figure 7A). It was hypothesized that the presence of bile salts could lead to membrane disruption by these surfactants and galactolipid substrate dispersion in water in the form of mixed micelles. Indeed, we have shown that NaTDC has an impact on the CRF membrane with an increased fluidity of acyl chains (Figure 6) and presumably an interaction with membranes proteins suggested by a decrease in absorbance of amide bands (Figures 5 and S4). We hypothesized that this decrease in absorbance could reflect the interaction between NaTDC and proteins and the formation of protein/NaTDC/lipid aggregates.

Nevertheless, the activity of GPLRP2 on CRF galactolipids was also shown in the absence of bile salts (7B), which demonstrated that GPLRP2 can access its galactolipid substrate in CRF membranes without the need of an interaction with bile salts. Moreover, the action of GPLRP2 on CRF in the absence of bile salts was characterized by a higher specific

activity (Table 2) and the percent of galactolipid fatty acid released reached 100% (Figure 7B). This implies that fatty acids from both sn-1 and sn-2 positions of galactolipids were released as observed during lipolysis of the model C8-MGDG micelles. Thus, PLRP2 is tailored for the total release of fatty acids from dietary galactolipids present in the chloroplast of vegetables. PLRP2 is present in human pancreatic juice (HPJ), what certainly explains the efficient digestion of galactolipids of CRF from spinach leaves and pea vine field residue observed in a previous study (Wattanakul et al., 2019). Further studies with whole plant leaves are now required for a better understanding of galactolipid digestibility.

The direct action of GPLRP2 on CRF galactolipids was not expected from the previous characterization of this enzyme. Indeed, studies with galactolipid and phospholipid monomolecular films (Hjorth et al., 1993) have shown the dependency of enzyme activity on surface pressure and optimum activities at low surface pressure. It was thus likely that GPLRP2, but also human PLRP2, could not hydrolyze galactolipids and phospholipids at the lateral surface pressure of natural membranes (30 mN/m) (Amara et al., 2013). Moreover, we have shown that GPLRP2 does not interact with and does not hydrolyze liposome of DPPC, while it is active on mixed micelles of the same phospholipids (Mateos-Diaz et al., 2018a).

CRF lipolysis by GPLRP2 in the absence of NaTDC, was accompanied by an increase in absorbance of the amide I' band, more precisely amide I' of β turn, random coil and β sheet structures. This increase in absorbance may have been caused by the disappearance of protein-galactolipid interactions and/or the appearance of interactions between proteins and other compounds, such as the proteins themselves or the lipolysis products (lyso-galactolipids and FFA) generated by GPLRP2. Since lyso-galactolipids are polar, it would not be surprising if they bound to proteins in the same way as galactolipids. FFAs are also known to interact with chloroplast proteins and modify their tertiary structures (Molotkovsky and Zheskova, 1965).

TLC analysis of CRF lipolysis confirmed the ability of GPLRP2 to hydrolyze chloroplasts without the presence of NaTDC. However, lipolysis seems less advanced in the absence than in the presence of NaTDC (Figure 8B), suggesting an overestimation by FTIR of the amount of FFA released during lipolysis of CRF in the absence of NaTDC. This may result from the fact that the FFA calibration curve was established with ALA in the presence of NaTDC. Indeed this later was required to ensure ALA dispersion in water.

4.5 Conclusion

FTIR transmission spectroscopy allowed quantitative measurement of the lipolysis of galactolipids by PLRP2, *in situ* and in real time. Using mixed micelles of a medium chain galactolipid (C8-MGDG) and bile salts (NaTDC) in D₂O as a model system, the concentrations of the residual substrate and lipolysis products were estimated from the carbonyl and carboxylate vibration bands after calibration with reference standards. The results were validated by TLC analysis after lipid extraction. *In situ* FTIR measurement performed in a 50- μ L liquid cell allowed monitoring the lipolysis reaction with a low amount of substrate, no sampling and no lipid extraction step. With more complex substrates like natural MGDG with long chain unsaturated FAs and intact chloroplasts isolated from spinach leaves, it was not possible to quantify all lipolysis products by FTIR. Nevertheless, the carboxylate vibration band allowed quantifying FFA released by PLRP2 using a calibration curve established with ALA dispersed in mixed micelles with bile salts. It was thus possible to estimate the specific activity of PLRP2 on all the substrates tested. Interestingly, all specific activities were in the same order of magnitude with values ranging from 133 ± 29 U/mg on CRF galactolipids to 492 ± 30 U/mg on LC-MGDG and 727 ± 67 U/mg on C8-MGDG. The highest values were obtained with galactolipids in mixed micelles with bile salts, in agreement with previous studies on the galactolipase activity of PLRP2 (Amara et al.,

2010). However, we have shown for the first time the direct action of PLRP2 on the galactolipids of chloroplast membranes without the need for bile salts. PLRP2 can therefore access to galactolipids present in bilayers and not only into micelles. Moreover, an almost complete release of FA from chloroplast galactolipids was observed, what fits with the ability of PLRP2 to release the two FAs present in C8-MGDG. These findings provide new insights into the substrate specificity of PLRP2 and further support its major contribution to galactolipid digestion in mammalian species.

Declaration of competing interest

The authors declare that there are no conflicts of interest.

Author contribution

Moulay Sahaka was involved in the conception and design of the study, in acquisition, analysis and interpretation of data, in drafting the article and revising it critically for important intellectual content. Eduardo Mateos-Diaz, Sawsan Amara and Jutarat Wattanakul were involved in acquisition, analysis and interpretation of data, and revising the article critically for important intellectual content. Dominique Lafont was involved in the chemical synthesis of C8-MGDG. David Gray, Brigitte Gontero, H el ene Launay were involved in revising the article critically for important intellectual content. Fr ed eric Carri ere was involved in the conception and design of the study, in analysis and interpretation of data, in drafting the article and revising it critically for important intellectual content. All authors were involved in the final approval of the version to be submitted.

Funding

This work received the financial support of Agence Nationale de la Recherche (France) in the framework of the GALACTOLIPASE project (ANR-09-CP2D-06-01).

Acknowledgements

The PhD thesis of Moulay Sahaka was supported by a fellowship from Aix Marseille Université, France. The PhD thesis of Miss Jutarat Wattanakul was supported by Thai Royal Government, Thailand.

References

- Amara, S., 2011. Etude de l'activité galactolipase des lipases pancréatiques apparentées de type 2 (PLRP2) (These de doctorat). Aix-Marseille 2.
- Amara, S., Barouh, N., Lecomte, J., Lafont, D., Robert, S., Villeneuve, P., De Caro, A., Carrière, F., 2010. Lipolysis of natural long chain and synthetic medium chain galactolipids by pancreatic lipase-related protein 2. *Biochimica et Biophysica Acta (BBA) - Molecular and Cell Biology of Lipids* 1801, 508–516. <https://doi.org/10.1016/j.bbalip.2010.01.003>
- Amara, S., Lafont, D., Fiorentino, B., Boullanger, P., Carrière, F., De Caro, A., 2009. Continuous measurement of galactolipid hydrolysis by pancreatic lipolytic enzymes using the pH-stat technique and a medium chain monogalactosyl diglyceride as substrate. *Biochimica et Biophysica Acta (BBA) - Molecular and Cell Biology of Lipids* 1791, 983–990. <https://doi.org/10.1016/j.bbalip.2009.05.002>
- Amara, S., Lafont, D., Parsiegla, G., Point, V., Chabannes, A., Rousset, A., Carrière, F., 2013. The galactolipase activity of some microbial lipases and pancreatic enzymes. *European Journal of Lipid Science and Technology* 115, 442–451. <https://doi.org/10.1002/ejlt.201300004>
- Barth, A., Zscherp, C., 2002. What vibrations tell about proteins. *Quart. Rev. Biophys.* 35, 369–430. <https://doi.org/10.1017/S0033583502003815>
- Belhaj, I., Amara, S., Parsiegla, G., Sutto-Ortiz, P., Sahaka, M., Belghith, H., Rousset, A., Lafont, D., Carrière, F., 2018. Galactolipase activity of *Talaromyces thermophilus* lipase on galactolipid micelles, monomolecular films and UV-absorbing surface-coated substrate. *Biochimica et Biophysica Acta (BBA) - Molecular and Cell Biology of Lipids* 1863, 1006–1015. <https://doi.org/10.1016/j.bbalip.2018.05.016>
- Blume, A., Huebner, W., Messner, G., 1988. Fourier transform infrared spectroscopy of ¹³C:O labeled phospholipids hydrogen bonding to carbonyl groups. *Biochemistry* 27, 8239–8249. <https://doi.org/10.1021/bi00421a038>
- Bril, C., Van der Horst, D.J., Poort, S.R., Thomas, J.B., 1969. Fractionation of spinach chloroplasts with sodium deoxycholate. *Biochimica et Biophysica Acta (BBA) - Bioenergetics* 172, 345–348. [https://doi.org/10.1016/0005-2728\(69\)90081-4](https://doi.org/10.1016/0005-2728(69)90081-4)
- Carrière, F., Withers-Martinez, C., van Tilbeurgh, H., Rousset, A., Cambillau, C., Verger, R., 1998. Structural basis for the substrate selectivity of pancreatic lipases and some related proteins. *Biochimica et Biophysica Acta (BBA) - Reviews on Biomembranes* 1376, 417–432. [https://doi.org/10.1016/S0304-4157\(98\)00016-1](https://doi.org/10.1016/S0304-4157(98)00016-1)

- Ceccaldi, M., Goldman, M., Roth, E., 1956. Le spectre d'absorption des mélanges H₂O-D₂O à l'état liquide entre 0,8 μ et 30 μ . *Spectrochimica Acta* 11, 623–631.
[https://doi.org/10.1016/S0371-1951\(56\)80105-7](https://doi.org/10.1016/S0371-1951(56)80105-7)
- de Jongh, H.H.J., Goormaghtigh, E., Ruyschaert, J.-M., 1997. Amide-Proton Exchange of Water-Soluble Proteins of Different Structural Classes Studied at the Submolecular Level by Infrared Spectroscopy. *Biochemistry* 36, 13603–13610.
<https://doi.org/10.1021/bi971337p>
- El Alaoui, M., Soullère, L., Noiriél, A., Popowycz, F., Khatib, A., Queneau, Y., Abousalham, A., 2016. A continuous spectrophotometric assay that distinguishes between phospholipase A₁ and A₂ activities. *J. Lipid Res.* 57, 1589–1597.
<https://doi.org/10.1194/jlr.D065961>
- Fauvel, J., Bonnefis, M.-J., Sarda, L., Chap, H., Thouvenot, J.-P., Douste-Blazy, L., 1981. Purification of two lipases with high phospholipase A1 activity from guinea-pig pancreas. *Biochimica et Biophysica Acta (BBA) - Lipids and Lipid Metabolism* 663, 446–456. [https://doi.org/10.1016/0005-2760\(81\)90173-9](https://doi.org/10.1016/0005-2760(81)90173-9)
- Goormaghtigh, E., Cabiaux, V., Ruyschaert, J.-M., 1994. Determination of Soluble and Membrane Protein Structure by Fourier Transform Infrared Spectroscopy, in: Hilderson, H.J., Ralston, G.B. (Eds.), *Physicochemical Methods in the Study of Biomembranes, Subcellular Biochemistry*. Springer US, Boston, MA, pp. 329–362.
https://doi.org/10.1007/978-1-4615-1863-1_8
- Hjorth, A., Carrière, F., Cudrey, C., Wöldike, H., Boel, E., Lawson, D.M., Ferrato, F., Cambillau, C., Dodson, G.G., Thim, L., 1993. A structural domain (the lid) found in pancreatic lipases is absent in the guinea pig (phospho)lipase. *Biochemistry* 32, 4702–4707. <https://doi.org/10.1021/bi00069a003>
- Kaufhold, D., Fagaschewski, J., Sellin, D., Strompen, S., Liese, A., Hilterhaus, L., 2014. Novel μ -membrane module for online determination of the free fatty acid content in the dispersed phase of oil-in-water emulsions. *Anal Bioanal Chem* 406, 3157–3166.
<https://doi.org/10.1007/s00216-014-7740-9>
- Khaskheli, A.A., Talpur, F.N., Ashraf, M.A., Cebeci, A., Jawaid, S., Afridi, H.I., 2015. Monitoring the *Rhizopus oryzae* lipase catalyzed hydrolysis of castor oil by ATR-FTIR spectroscopy. *Journal of Molecular Catalysis B: Enzymatic* 113, 56–61.
<https://doi.org/10.1016/j.molcatb.2015.01.002>
- Kong, J., Yu, S., 2007. Fourier Transform Infrared Spectroscopic Analysis of Protein Secondary Structures. *Acta Biochim Biophys Sinica* 39, 549–559.
<https://doi.org/10.1111/j.1745-7270.2007.00320.x>
- Lafont, D., Carrière, F., Ferrato, F., Boullanger, P., 2006. Syntheses of an α -d-Gal-(1→6)- β -d-Gal diglyceride, as lipase substrate. *Carbohydrate Research* 341, 695–704.
<https://doi.org/10.1016/j.carres.2006.01.021>
- Levin, I.W., Mushayakarara, E., Bittman, R., 1982. Vibrational assignment of the sn-1 and sn-2 chain carbonyl stretching modes of membrane phospholipids. *J. Raman Spectrosc.* 13, 231–234. <https://doi.org/10.1002/jrs.1250130306>
- Lewis, R.N., McElhaney, R.N., 1993. Studies of mixed-chain diacyl phosphatidylcholines with highly asymmetric acyl chains: a Fourier transform infrared spectroscopic study of interfacial hydration and hydrocarbon chain packing in the mixed interdigitated gel

- phase. *Biophysical Journal* 65, 1866–1877. [https://doi.org/10.1016/S0006-3495\(93\)81251-7](https://doi.org/10.1016/S0006-3495(93)81251-7)
- Mateos-Diaz, E., Bakala N’Goma, J.-C., Byrne, D., Robert, S., Carrière, F., Gaussier, H., 2018a. IR spectroscopy analysis of pancreatic lipase-related protein 2 interaction with phospholipids: 1. Discriminative recognition of mixed micelles versus liposomes. *Chem. Phys. Lipids* 211, 52–65. <https://doi.org/10.1016/j.chemphyslip.2017.02.005>
- Mateos-Diaz, E., Sutto-Ortiz, P., Sahaka, M., Rodriguez, J.A., Carrière, F., 2018b. IR spectroscopy analysis of pancreatic lipase-related protein 2 interaction with phospholipids: 3. Monitoring DPPC lipolysis in mixed micelles. *Chemistry and Physics of Lipids* 211, 77–85. <https://doi.org/10.1016/j.chemphyslip.2017.11.009>
- Mielczarski, J.A., Cases, J.M., Bouquet, E., Barres, O., Delon, J.F., 1993a. Nature and structure of adsorption layer on apatite contacted with oleate solution. 1. Adsorption and Fourier transform infrared reflection studies. *Langmuir* 9, 2370–2382. <https://doi.org/10.1021/la00033a020>
- Mielczarski, J.A., Cases, J.M., Tekely, P., Canet, D., 1993b. Nature and structure of adsorption layer on apatite contacted with oleate solutions. 2. In situ and ex situ Fourier transform infrared, NMR, and x-ray photoelectron spectroscopy studies. *Langmuir* 9, 3357–3370. <https://doi.org/10.1021/la00036a007>
- Mizuguchi, M., Nara, M., Kawano, K., Nitta, K., 1997. FT-IR study of the Ca²⁺-binding to bovine α -lactalbumin: Relationships between the type of coordination and characteristics of the bands due to the Asp COO⁻ groups in the Ca²⁺-binding site. *FEBS Letters* 417, 153–156. [https://doi.org/10.1016/S0014-5793\(97\)01274-X](https://doi.org/10.1016/S0014-5793(97)01274-X)
- Molotkovsky, Y.G., Zheskova, I.M., 1965. The influence of heating on the morphology and photochemical activity of isolated chloroplasts. *Biochemical and Biophysical Research Communications* 20, 411–415. [https://doi.org/10.1016/0006-291X\(65\)90592-9](https://doi.org/10.1016/0006-291X(65)90592-9)
- Müller, J.J., Baum, S., Hilterhaus, L., Eckstein, M., Thum, O., Liese, A., 2011. Simultaneous Determination of Mono-, Di-, and Triglycerides in Multiphase Systems by Online Fourier Transform Infrared Spectroscopy. *Anal. Chem.* 83, 9321–9327. <https://doi.org/10.1021/ac2018662>
- Müller, J.J., Neumann, M., Scholl, P., Hilterhaus, L., Eckstein, M., Thum, O., Liese, A., 2010. Online Monitoring of Biotransformations in High Viscous Multiphase Systems by Means of FT-IR and Chemometrics. *Anal. Chem.* 82, 6008–6014. <https://doi.org/10.1021/ac100469t>
- Natalello, A., Sasso, F., Secundo, F., 2013. Enzymatic transesterification monitored by an easy-to-use Fourier transform infrared spectroscopy method. *Biotechnology Journal* 8, 133–138. <https://doi.org/10.1002/biot.201200173>
- O’Connor, C.J., Cleverly, D.R., 1994. Fourier-transform infrared assay of bile salt-stimulated lipase activity in reversed micelles. *J. Chem. Technol. Biotechnol.* 61, 209–214. <https://doi.org/10.1002/jctb.280610305>
- Sahaka, M., Amara, S., Lecomte, J., Rodier, J.-D., Lafont, D., Villeneuve, P., Gontero, B., Carrière, F., 2021. Quantitative monitoring of galactolipid hydrolysis by pancreatic lipase-related protein 2 using thin layer chromatography and thymol-sulfuric acid derivatization. *Journal of Chromatography B* 1173, 122674. <https://doi.org/10.1016/j.jchromb.2021.122674>

- Sahaka, M., Amara, S., Wattanakul, J., Gedi, M.A., Aldai, N., Parsiegla, G., Lecomte, J., Christeller, J.T., Gray, D., Gontero, B., Villeneuve, P., Carrière, F., 2020. The digestion of galactolipids and its ubiquitous function in Nature for the uptake of the essential α -linolenic acid. *Food Funct.* 11, 6710–6744. <https://doi.org/10.1039/D0FO01040E>
- Sias, B., Ferrato, F., Grandval, P., Lafont, D., Boullanger, P., De Caro, A., Leboeuf, B., Verger, R., Carrière, F., 2004. Human Pancreatic Lipase-Related Protein 2 Is a Galactolipase †. *Biochemistry* 43, 10138–10148. <https://doi.org/10.1021/bi049818d>
- Snabe, T., Petersen, S.B., 2002. Application of infrared spectroscopy (attenuated total reflection) for monitoring enzymatic activity on substrate films. *Journal of Biotechnology* 95, 145–155. [https://doi.org/10.1016/S0168-1656\(02\)00005-6](https://doi.org/10.1016/S0168-1656(02)00005-6)
- Snyder, R.G., Strauss, H.L., Elliger, C.A., 1982. Carbon-hydrogen stretching modes and the structure of n-alkyl chains. 1. Long, disordered chains. *J. Phys. Chem.* 86, 5145–5150. <https://doi.org/10.1021/j100223a018>
- Stöbener, A., Fabuel Ortega, M., Bolten, C.J., Ananta, E., Nalur, S., Liese, A., 2020. *In situ* monitoring of the biocatalysed partial hydrolysis of cocoa butter and palm oil fraction. *Int J Food Sci Technol* 55, 1265–1271. <https://doi.org/10.1111/ijfs.14366>
- Vlachos, N., Skopelitis, Y., Psaroudaki, M., Konstantinidou, V., Chatzilazarou, A., Tegou, E., 2006. Applications of Fourier transform-infrared spectroscopy to edible oils. *Analytica Chimica Acta* 573–574, 459–465. <https://doi.org/10.1016/j.aca.2006.05.034>
- Walde, P., Luisi, P.L., 1989. A continuous assay for lipases in reverse micelles based on Fourier transform infrared spectroscopy. *Biochemistry* 28, 3353–3360. <https://doi.org/10.1021/bi00434a034>
- Wattanakul, J., Sahaka, M., Amara, S., Mansor, S., Gontero, B., Carrière, F., Gray, D., 2019. In vitro digestion of galactolipids from chloroplast-rich fraction (CRF) of postharvest, pea vine field residue (haulm) and spinach leaves. *Food Funct.* 10, 7806–7817. <https://doi.org/10.1039/C9FO01867K>
- Wieser, H., Danyluk, M., 1972. Infrared Band Progressions in the CH₂ Scissoring Region and the Ring Puckering Vibration of Trimethylene Oxide and some Deuterated Analogs. *Can. J. Chem.* 50, 2761–2770. <https://doi.org/10.1139/v72-442>
- Withers-Martinez, C., Carrière, F., Verger, R., Bourgeois, D., Cambillau, C., 1996. A pancreatic lipase with a phospholipase A1 activity: crystal structure of a chimeric pancreatic lipase-related protein 2 from guinea pig. *Structure* 4, 1363–1374. [https://doi.org/10.1016/S0969-2126\(96\)00143-8](https://doi.org/10.1016/S0969-2126(96)00143-8)
- Yan, W.-H., Strauss, H.L., Snyder, R.G., 2000. Conformation of the Acyl Chains in Diacylphospholipid Gels by IR Spectroscopy. *J. Phys. Chem. B* 104, 4229–4238. <https://doi.org/10.1021/jp993944n>
- Yu, D., Huang, G., Xu, F., Wang, M., Liu, S., Huang, F., 2014. Triton X-100 as an effective surfactant for the isolation and purification of photosystem I from *Arthrospira platensis*. *Photosynth Res* 120, 311–321. <https://doi.org/10.1007/s11120-014-9988-5>
- Zagonel, G.F., Peralta-Zamora, P., Ramos, L.P., 2004. Multivariate monitoring of soybean oil ethanolysis by FTIR. *Talanta* 63, 1021–1025. <https://doi.org/10.1016/j.talanta.2004.01.008>

Figure legends

Figure 1. *Representative spectra of spinach CRF, natural LC MGDG, synthetic C8-MGDG, ALA, OA and PA. Acyl chain, carbonyl, carboxylate and amide vibrations are attributed in panels B, C, D and E, respectively. All spectra were recorded in the presence of NaTDC, at pD 8 and 37 °C.*

Figure 2. *Spectra of carbonyl and carboxylate vibrations during the hydrolysis of C8-MGDG–NaTDC and LC MGDG–NaTDC micelles. Panel A, B and C show the evolution of the ‘raw’ spectra, while panels A’, B’ and C’ panels show the difference spectra, obtained from the subtraction of the initial spectrum. The hydrolysis was monitored for 120 min at 5 min intervals, at 37°C and pD 8. GPLRP2 concentration was 50 nM.*

Figure 3. *Spectra of carbonyl ($\nu_{C=O}$) and carboxylate ($\nu_s\text{COO}^-$ and $\nu_{as}\text{COO}^-$) vibrations of C8-MGDG, C8-MGMG, OA, ALA and PA standards, at different concentrations. All lipids were solubilised in mixed micelles with NaTDC. The lipid concentration ranges from 0 to 50 mM for C8-MGDG and OA, from 0 to 26 mM for C8-MGMG and from 0 to 15 mM for ALA. NaTDC concentration was 56 mM for C8-MGDG, C8-MGMG and OA, and 30 mM for ALA. IR spectra were recorded at 37 °C and pD 8.*

Figure 4. *Time-course variations in the concentrations of lipolysis products and residual substrate during the hydrolysis of C8-MGDG–NaTDC (A, B, C) and LC MGDG–NaTDC micelles (D) by GPLRP2. Substrate concentrations were 50 mM for C8-MGDG mixed with NaTDC and 22.5 mM for LC-MGDG. Reactions were catalyzed using either 100 nM (panels A and B) or 50 nM (panels C and D) GPLRP2, at pD 8 and 37 °C. Experiments were monitored using either FTIR spectroscopy (panels A, C and D) or TLC-densitometry (Panel B). Values are means \pm SD (n =3).*

Figure 5. *Difference spectra of carbonyl, carboxylate and amide vibrations during the lipolysis of CRF, in the presence (panel A, B and C) and absence (panel A', B' and C') of NaTDC. Lipolysis was catalyzed by 50 nM GPLRP2, at 37°C and pD 8.*

Figure 6. *Spectra of CRF acyl chain vibrations, in the absence (green line) and presence (red line) of NaTDC, at 37°C and pD 8 (panel A). Microscopic images of isolated chloroplasts (CRF), rehydrated in the presence of NaTDC (panel B) and chloroplasts inside spinach leave cells (panel C).*

Figure 7. *Time-course variations in the concentration of FFA during the hydrolysis of spinach CRF, in the presence (panel A) and absence (panel B) of NaTDC. Reactions were catalysed by 50 nM GPLRP2. Experiments were performed at pD 8 and 37 °C. Values are means \pm SD (n =3). FFA levels are also expressed in % of the total FAs initially present in CRF galactolipids, with the scale shown on the right for each panel.*

Figure 8. *TLC analysis of CRF hydrolysis, in the presence and in absence of NaTDC. The hydrolysis was catalysed by 50 nM GPLRP2. The incubation was performed during 1h, at pH 8 and 37°C. Substrate and products were extracted using Folch method, separated by TLC and derivatized using thymol-sulfuric acid reagent.*

Figure 9. *Reaction scheme for the hydrolysis of MGDG catalyzed by GPLRP2. 1-sn-MGMG and 2-sn-MGMG are monogalactosyl mono-octanoylglycerol with one acyl chain at positions sn-1 and sn-2 of the glycerol backbone, respectively. MGG is monogalactosylglycerol.*

Table 1. Molar extinction coefficients (ϵ , $M^{-1} \text{ cm}^{-1}$) of C8-MGDG, C8-MGMG, OA and ALA from IR absorbance. The ϵ -values represent the slope of the standard calibration curves of IR absorbance of C8-MGDG, C8-MGMG, OA and ALA at different wavenumbers, at pD 8 (see Figure S2). All IR measurements were performed in D_2O , in the presence of NaTDC, at pD 8 and 37 °C.

Compound	Vibration band	Wavenumber	ϵ	R^2
C8-MGDG	$\nu C=O$	1744 cm^{-1}	478.1	0.998
		1722 cm^{-1}	454.4	0.999
		1682 cm^{-1}	38.6	0.929
C8-MGMG	$\nu C=O$	1744 cm^{-1}	134.8	0.988
		1722 cm^{-1}	302.7	0.998
		1682 cm^{-1}	33.3	0.957
OA	$\nu C=O$	1744 cm^{-1}	22.0	0.928
		1722 cm^{-1}	33.5	0.946
		1682 cm^{-1}	89.2	0.996
	$\nu_{as}COO^-$	1553 cm^{-1}	751.8	0.997
	ν_sCOO^-	1408 cm^{-1}	227.6	0.996
ALA	$\nu_{as}COO^-$	1555 cm^{-1}	595	0.967
	ν_sCOO^-	1407 cm^{-1}	204.2	0.988

Table 2: Specific activities (U/mg or μ mole FFA per min per mg of enzyme) of GPLRP2 on C8-MGDG-NaTDC micelles, LC-MGDG-NaTDC micelles and spinach CRF with and without NaTDC. The activities were calculated using the amounts of fatty acid released during 10 minutes from the start of the reaction (0-10 min) or from the fifth minute of reaction (5-15 min). The reactions were performed at 37 °C and pD 8.

	Method	GPLRP2 Concentration	Reaction interval used for specific activity calculation	Specific Activity (U/mg)
C8-MGDG	TLC	100 nM	0-10 min	981 \pm 97
	IR	100 nM	0-10 min	727 \pm 67
		50 nM	0-10 min	439 \pm 125
LC MGDG	IR	50 nM	0-10 min	492 \pm 30
			5-15 min	166 \pm 9
Spinach CRF with NaTDC	IR	50 nM	5-15 min	89 \pm 7
Spinach CRF without NaTDC	IR	50 nM	5-15 min	133 \pm 29